Journal of Pharmaceutical Innovation (2019) 14:194–205
https://doi.org/10.1007/s12247-018-9349-6

ORIGINAL ARTICLE

Manufacturing of Pharmaceuticals by Impregnation of an Active Pharmaceutical Ingredient onto a Mesoporous Carrier: Impact of Solvent and Loading

Thamer A Omar[1] · Sarang Oka[2] · Fernando J. Muzzio[2] · Benjamin J. Glasser[2]

Abstract

Purpose In this study, an active pharmaceutical ingredient (API) was impregnated onto a mesoporous carrier (excipient) in a fluidized bed. Impregnating APIs in porous carriers has the potential to simplify the drug substance development process and leads to the elimination of the blending and granulation unit operations. Impregnation and drying occur simultaneously in fluidized-bed impregnation, and this method precludes several challenges encountered in other impregnation methods. Furthermore, the process ensures a uniform distribution of APIs within the porous carriers. This method also allows for a variety of solvents to be used in the impregnation.

Methods Using a batch fluidized-bed dryer, impregnation of acetaminophen (APAP) onto a magnesium/aluminum metasilicate (Neusilin ^{R}) was studied. Water and methanol were used as transport solvents to impregnate different loadings (*w*/*w*) of APAP, namely, ranging from 24 to 0.1%.

Results Uniformity tests indicated that APAP loadings of all impregnated products are close to their target loadings across carrier size classes. Tests before and after impregnation showed that there were no changes observed in the physical properties of the carrier, such as particle size, compressibility, and flow properties. X-ray diffraction (XRD) and differential scanning calorimetry (DSC) analysis performed on the samples indicated that the low loadings APAP was present in the carrier pores in its amorphous state. At high loadings, we observed that APAP was mainly present in its amorphous state, however, some degree of crystallinity was observed. Lastly, dissolution tests on the impregnated product showed enhanced dissolution rates in acidic media, and comparable dissolution rate in de-ionized (DI) water, compared to the pure drug crystals.

Conclusion Our results show that the method of fluidized-bed impregnation yields a product with high uniformity and overcomes several challenges presented by traditional physical blends.

Keywords Impregnation · Fluidized bed · Amorphous · Porous carriers · Drying · Solid dosage forms

Introduction

Impregnation can be defined as a process of placing chemical substances (such as drugs) inside porous carriers. Recently, there has been an increasing interest in the use of mesoporous carriers (MC) in drug delivery [1, 2] because of their amenable physical properties such as a narrow particle-size distribution, high surface area, good flow properties, and small pore sizes with narrow distribution [3]. The high surface area of these carriers allows them to absorb several compounds, including poorly flowing materials like oily drugs. Since, these compounds are completely embedded within the porous carriers, the physical properties of the impregnated products are identical to the carrier, thereby facilitating their handling and further processing [4, 5]. Moreover, the drug within the pores of the MC mainly exists in an amorphous form, which is known to improve its dissolution [6]. Very small pore sizes of the MC, for example Neusilin US2, result in confining of the drug, which limits the drug's mobility and inhibits the drug's

---

✉ Benjamin J. Glasser
bglasser@rutgers.edu

[1] Ernest Mario School of Pharmacy, Rutgers, The State University of New Jersey, 160 Frelinghuysen Road, Piscataway, NJ 08854, USA

[2] Department of Chemical and Biochemical Engineering, Rutgers, The State University of New Jersey, 98 Brett Road, Piscataway, NJ 08854, USA

recrystallization inside these pores [6, 7]. Accordingly, impregnation of drugs into a MC can improve some crucial properties of the drugs such as its dissolution behavior [8]. In contrast, other pharmaceutical manufacturing processes, which were designed to improve drug properties, involve many challenges in terms of processing steps, and controlling product quality [9, 10]. The production of drug-carrier complexes that are independent of the physical properties of the active ingredient, along with its dissolution behavior, makes it amenable for development as a solid oral dose product. Thus, one aim of this work is preserving the physical and chemical properties of the composite, which is considered as a benefit in terms of the drug properties. Also, mesoporous carriers can be used to reduce the drug's adverse effects. For example, oxybenzone, which is used in sunscreen preparations, was successfully loaded into a mesoporous carrier (MCM-41) to reduce its side effects [11]. A thorough discussion about the new applications of mesoporous silicon dioxide and silicates in drug product development can be found in Qian and Borgner [12].

Lastly, impregnation eliminates the need for several intermediate processing steps, in both the drug substance and the drug product development routines. Drug substance and drug product development are intertwined processes, where drug product development completely depends on properties of the drug substance. Drug product development, irrespective of the manufacturing route, is sensitive to change in the properties of the drug substance. Thus, enabling superior control of the drug substance attributes is beneficial for a successful drug product development. The monitoring and control of physicochemical properties of the drug substance is not a simple task, and involves many unit operations. In general, it begins with choosing the state of the drug substance—crystalline or amorphous. This is followed by working to achieve the desired physical properties. Crystalline drug substances are relatively stable and pure, and are preferentially used in manufacturing of solid dosage form over the amorphous form of drug substance. However, achieving the desired properties of the crystalline drug substance is challenging and involves manipulating the crystallization process variables, and controlling the filtration process [13]. Amorphous form of drugs, albeit being good alternatives, is usually physically unstable. It is also difficult to control their physical properties during drug substance and drug product development. As previously mentioned, using mesoporous carriers improves the physical stability of amorphous drug substances [6, 7] and facilitates control over some of the essential drug substance attributes such as particle size, flow properties, and dissolution behavior.

Consequently, several loading methods have been developed for incorporating crystalline drugs into MC. Loading drugs into these carriers can be done by co-milling [6], melt adsorption using hot-melt extrusion [14], spontaneous evaporation and sublimation [15, 16], co-spray drying [17], and wet impregnation [18, 19]. However, several of the aforementioned techniques exhibit drawbacks and manufacturing challenges. For instance, both co-milling and hot-melt extrusion may lead to a change in the physical structure of both the drug due to elevation of the drug's temperature above its glass transition temperature. In addition, some drugs show polymorphism at high temperatures, which can lead to loss of the drug's stability and therapeutic effects. Furthermore, co-grinding can also change the morphology of both, the drug and the carrier [6, 20], resulting in products with poor flowability, and poor compactability. The spontaneous evaporation and sublimation method was also found to be challenging from a process configuration and scale-up perspective. For instance, it is difficult to control process parameters, ensure product quality, and achieve amenable scale-up of a porous dispersion, which was prepared using flash evaporation [21]. On the other hand, wet impregnation has been found to be comparatively successful. It can be achieved using several different approaches. The most routine approach involves dissolving the drug in a suitable solvent and mixing this solution with a porous carrier, followed by filtering of the resultant impregnated product [1, 18, 19]. One drawback of this method is the difficulty in achieving an accurate desired drug load, and the large equilibration and filtration cycle times. Wet impregnation can also be performed by a method called "incipient wet impregnation," which includes mixing the drug solution with the porous carrier followed by evaporating the organic solvent from the mixture. The mixing and drying are usually repeated more than once [22]. However, like standard wet impregnation, this method is slow and often results in non-homogeneous loading of the carrier.

Recently, Grigorov et al. [23] attempted a new method to impregnate drugs into porous carriers. This method involves spraying the drug solution onto porous carriers within a fluidized bed (FB). Impregnation and drying occur simultaneously and the method enables one to achieve different drug loadings independent of the drug's solubility. This approach eliminated the need to repeat spraying and drying cycles, unlike the wet impregnation methods. Furthermore, the method resulted in a uniform distribution of the API within the carrier, thereby resulting in a product with excellent blend uniformity and a narrow particle-size distribution. Moreover, this operation is easy to scale-up for production on large scales. Fluidized-bed impregnation is a single step process to load drug substances into a carrier and eliminates several operations from the drug substance development routine. In addition to the simplification of the drug substance development process, fluid bed impregnation eliminates the need for additional excipients to improve the flow properties. Also, some unit operations from product development like granulation that are necessary to improve drug flow properties can now be excluded from the development process. However, we may still need a blending step for product development such as blending of impregnated products with lubricants in the case of tablet production. Fluid bed impregnation is easy to integrate in a manufacturing train, and also lends itself to continuous processing.

While Grigorov et al. [8, 23] examined the impregnation of acetaminophen (APAP) in dibasic calcium phosphate and fenofibrate in Neusilin, they used a single solvent (methanol) to impregnate selected drugs in a single carrier material. It is of interest to look at the same drug in a different carrier and also look at the same drug with different solvents to see the effect of solvents. In this paper, we have examined the impregnation of APAP in Neusilin using both water and methanol. We compared the results of these two solvents to see what effects these solvents will have on the properties of impregnated products and their dissolution behaviors. In addition, our results for APAP in Neusilin can be compared to previous work for APAP in methanol impregnated in dibasic calcium phosphate. Thus, this work aims to test the robustness of the fluidized-bed impregnation process, and its applicability for a variety of solvents. Impregnation of acetaminophen (APAP) onto a magnesium/aluminum metasilicate (Neusilin ^{R} US2 (NEU)) has been studied in a Mini-Glatt spray fluidized-bed dryer/granulator. Different APAP loadings have been investigated and the physical properties of the impregnated product have been thoroughly characterized.

Materials and Methods

Materials

Neusilin® US2 was purchased from Fuji Health Science Inc. (Burlington, NJ, USA). Methanol, B&J Brand® Multipurpose Grade (purity above 99%), was purchased from VWR International. Acetaminophen (Semi-fine) was obtained from Mallinckrodt (Raleigh, NC, USA).

Experimental Setup and Impregnation Procedure

Impregnation experiments were carried out in a Mini-GLATT fluidized-bed dryer/coater/granulator, equipped with a top spray nozzle (Glatt Inc., Ramsey NJ, USA). The procedure developed for fluidized-bed impregnation (FBI) consisted of the following steps: (1) Load fluidized-bed dryer with NEU (about 220 g) until the top spray nozzle is reached. Thus, during fluidization, the nozzle is located within the bed to reduce spray drying. (2) Run fluidized-bed dryer to a stable fluidization profile and adjust the inlet gas temperature to 80 °C. (3) Begin spraying the pure solvent (methanol or water). Spraying only pure solvent at the beginning is necessary to reach a steady state temperature of the product. (4) After achieving a steady state (constant product temperature), start spraying the APAP solution. The APAP solution is prepared by dissolving a desired quantity of APAP, based on the drug load, in pure methanol or DI water. Generally, we prefer the API concentration in the solvent to be as low as possible; if we add a large amount of drug in a short time, this may lead to poor blend uniformity. At the same time, if we make the API concentration extremely low, then the operation will take an unreasonable amount of time. So, we chose API concentrations that allow us to complete an experiment within a few hours and still obtain good blend uniformity. (5) Once the desired quantity of API is sprayed in solution form, spray pure solvent for 20 min. Spraying pure solvent after spraying the drug solution is essential to dissolve any APAP at the surface of NEU, and impregnate it. (6) Dry the impregnated product until the product temperature reaches 50 °C. (7) Cool down the product and discharge.

The resulting impregnated product was placed in a tray. Ten random samples were extracted from different locations in the tray. These samples were stored inside glass vials and used for the blend uniformity study. As previously mentioned, APAP was impregnated onto NEU for four different loadings (*w*/*w*), namely, 0.1, 1, 9, and 24% using methanol as a solvent, while it was impregnated using water at three different concentrations, namely, 0.1, 1, and 5%. Details of the experimental conditions and the process parameters are presented in Table 1.

Analytical Methods

The following analytical methods were employed in order to characterize the impregnated product and the pure carrier.

Microscopy and Particle-Size Distribution

Scanning electron microscopic pictures were captured using a Zeiss Sigma FE-scanning electron microscope. Particle-size distributions (PSD) of all materials were measured using a laser diffraction technique (Beckman Coulter LS 13320). The pattern of scattered light, as measured by intensity at various angles, was correlated to the particle-size distribution of a sample. The measurements were presented as volume percent as a function of the particle size. D_{10}, D_{50}, and D_{90} can be computed using the equipment software. Each

Table 1 Conditions for all fluidized-bed impregnation experiments

Products	Pump rate (ml/min)	Inlet gas pressure (bar)	Atomization pressure (bar)	Inlet gas temp. (°C)	Spray time of APAP (min)
Impregnated	4	0.1	0.2	80	162.5

measurement was performed in triplicate and the average value is shown in Table 2.

Shear Cell Tests

The flow properties of pure NEU and the impregnated product were measured using a FT-4 powder rheometer (Freeman Technology Inc., UK). The procedure includes four steps: conditioning, consolidation, pre-shearing, and shearing. Conditioning was accomplished by placing the testing powder into a glass cylinder. The powder bed was subjected to a helical rotating blade to produce a homogenous, reproducible state of the powder and eliminate any consolidation history. After that, a vented piston was used to achieve a desired consolidation state. The consolidating powder was pre-sheared to achieve a steady state at maximum shear stress. Then, this normal stress was reduced to a new normal stress and the sample was further sheared to achieve a yield point. The pre-shear procedure was repeated five times at different normal stresses to obtain the yield locus [24]. All experiments were performed in triplicate. More details about the procedure can be found in Freeman et al. [25].

Specific Surface Area and Pore Volume Distribution

Surface area (m^2/g) analysis was performed using nitrogen as the adsorbate using Autosorb1 (Quantachrome Instruments, USA). The specific surface area was determined using 7-point N_2 adsorption by the Brunauer-Emmett-Teller (BET) model [26]. The specific surface area was measured across a partial pressure range of 0.05–1, and using seven points. All samples were degassed for at least 18 h at 40 °C before the measurement.

Drug Loading and Blend Uniformity

Drug loading was measured using UV/visible spectroscopy (Varian Cary 50 Bio, Agilent Technologies, USA). As mentioned previously, ten samples were extracted from each experiment. Ten samples were sufficient to obtain precise and representative blend uniformity results. Four hundred milligrams from each sample was placed in 100 ml conical flasks; and methanol was added till the 100 ml mark. This dispersion was sonicated for 40 min and left overnight at room temperature to ensure a complete extraction of APAP from NEU. Samples were then withdrawn from each flask using a millipore (0.45 μm) syringe filter. The UV readings at $\lambda = 247.5$ nm were acquired and analyzed to quantify the amount of APAP in each sample. In order to quantify the measured absorbance, a calibration curve was built up by acquiring the UV absorbance of five different concentrations of APAP in methanol.

Consequently, the APAP loading of each sample, the mean, the standard deviation and the % relative standard deviation (% RSD) along with the confidence intervals (C.I.) of the measurements for each batch were computed using [27]:

$$\nu \in \left(\sqrt{\frac{(n-1)\, V^2}{(\chi/\mu)^2_{1-\alpha/2,n-1}}}, \sqrt{\frac{(n-1)\, V^2}{(\chi/\mu)^2_{\alpha/2,n-1}}} \right.$$

where $\boldsymbol{\nu}$ is the confidence interval; $\boldsymbol{V}$ is the expected value of the RSD measurement; $\boldsymbol{n-1}$ is the degree of freedom; $(\boldsymbol{\chi}/\boldsymbol{\mu})^{\mathbf{2}}$ is chi-on-mu-square, which is a statistical value, that can be obtained from a table for different significance levels and degrees of freedom.

X-Ray Powder Diffraction

X-ray powder diffraction patterns were obtained using a PANalytical X'pert, which was operated at 35 kV and 50 mA. The scan procedure included the following conditions: scan axis, gonio; scan range (°), 5–60; step size (°), 0.0131; number of points, 4188; scan mode: continuous; counting time (s), 4.845.

Raman Spectroscopy

Raman spectra were acquired using a RAMANRXN1™ (PhAT System™) from Kaiser Optical Systems, Inc., MI, USA. Before starting sample measurements, the device was calibrated using cyclohexane as a standard. Measurements were performed under the following conditions: laser wavelength at 785 nm; spectral

Table 2 Particle size of Neusilin and impregnated products. The results indicated that particle size of pure Neusilin is preserved after impregnation

Products (%)	Solvent	Mean (μm)	Median (μm)	S.D.	D_{10} (μm)	D_{90} (μm)
Pure NEU		129.1	128.4	56.72	55.10	205.6
0.1	DI water	127.6	126.0	55.21	55.94	202.6
1		130.7	129.3	55.78	59.01	205.9
5		132.6	133.0	54.2	61.45	204.6
0.1	Methanol	128.3	127.7	54.61	57.66	201.7
1		131.7	131.9	53.54	60.78	203
9		132.3	132.2	54.26	61.01	204.9
24		136.3	135.5	52.66	69.44	206.8

coverage from 150 to 1875 cm^{-1}; exposure time at 30 s; laser power of sample at 400 mW. Raman spectra were acquired for both impregnated and physical mixtures of 5%, 9%, and 24% APAP in NEU. Five percent, 9%, and 24% physical blends (*w*/*w*) of APAP and NEU were prepared using a Lab-RAM mixer (Resodyn™ Acoustic Mixers, Inc., USA) at 60% intensity for 3 min vibration time.

Differential Scanning Calorimetry

Differential scanning calorimetry (DSC) analysis was performed using a differential scanning calorimeter Q1000 by TA Instruments. The heat ramp of samples was from 0 to 210 °C, using nitrogen gas flowing at 50 ml/min. The heating rate of the samples was 10 °C /min. The sample masses were around 10 mg, and they were put in pin-hole aluminum pans before measurement.

Dissolution Behavior

Dissolution behavior of APAP from the impregnated product was tested using a 708-DS, 8-spindle, 8-vessel USP dissolution apparatus type II (paddle), with automated online UV-Vis measurement (Agilent Technologies). Dissolution tests were conducted on pure APAP and the impregnated product (equivalent 30 mg APAP). The experimental conditions were set as follows: 900 ml of DI water or 0.1 N HCl as a dissolution medium; agitation speed, 50 rpm; UV detection, $\lambda = 240$ nm for 0.1 N HCl, and $\lambda = 245$ nm for DI water; temperature, 37 °C. All experiments were performed in triplicate. In order to quantify the measured absorbance, a calibration curve was constructed (Abs = 66.038 × Conc., $R^2 = 0.9999$ for 0.1 N HCl; Abs = 64.935 × Conc., $R^2 = 0.9999$ for DI water) by measuring the UV absorbance for five different concentrations of APAP in the dissolution media.

Results and Discussion

Particle Size and SEM

The particle-size distribution (PSD) of the pure carrier and the impregnated product is shown in Table 2 and Fig. 1. It can be observed that the PSD of the pure NEU is almost identical to that of the impregnated product. The preservation of the particle-size distribution of the carrier and the absence of fines suggests the feasibility of impregnating drug products into porous carriers using fluidized beds.

The absence of fines, indicated by no significant change in the D_{10} (see Table 2), is also indicative of a gentle process, without major attrition of the carrier particles [6, 23].The creation of excessive fines during processing, and their subsequent presence in a formulation is generally undesirable. Presence of excessive fines in a formulation can lead to poor flow and dusting. What is also observed is that the mean particle size of the impregnated product lies between 128.3–136.3 μm. This makes them suitable for most oral solid dose unit operations. These products are also similar in particle size to a large number of the common pharmaceutical excipients. So, these impregnated products are compatible to mix with most pharmaceutical excipients, which are used in manufacturing of solid dosage forms. For instance, the mean particle size of lactose monohydrate—SuperTab® 11SD—and microcrystalline cellulose—Avicel pH 102—are 116 and 124 μm, respectively. This makes them amenable to physical homogenization with excipients, and alleviates segregation risk [28]. Furthermore, particle agglomeration or aggregation of the impregnated product was not observed. The D_{90} of the impregnated product is approximately the same as the D_{90} of the pure NEU.

SEM pictures of the pure and impregnated NEU are shown in Fig. 2. As can be seen in this figure, the impregnated products possess a spherical morphology, which is essential for

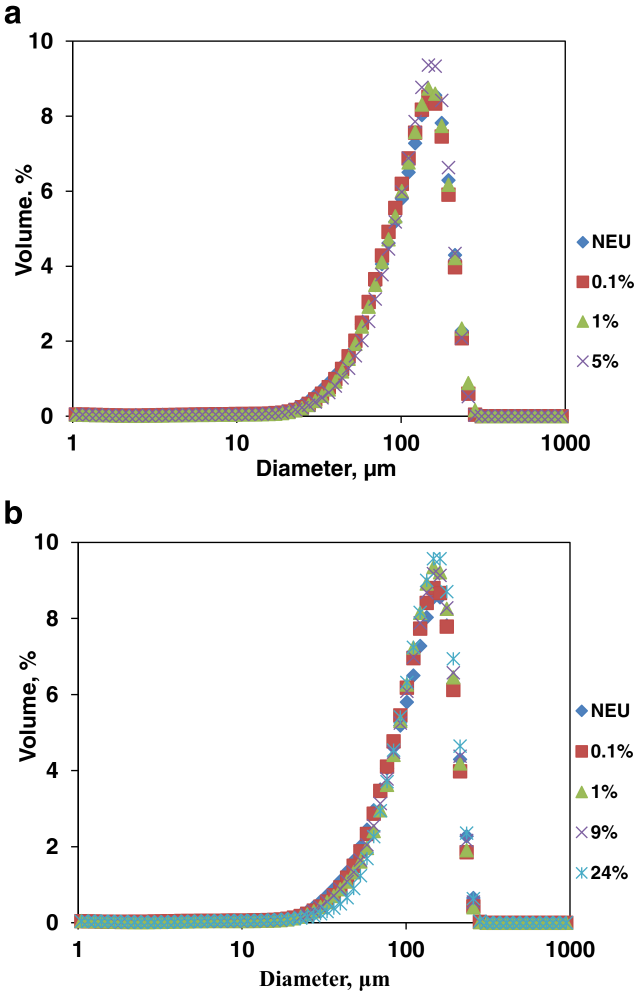

Fig. 1 Particle-size distribution comparison for **a** pure Neusilin (NEU) and impregnated products using DI water as a solvent and **b** pure NEU and impregnated products using methanol as a solvent. The PSD of pure NEU and the impregnated is comparable in both cases

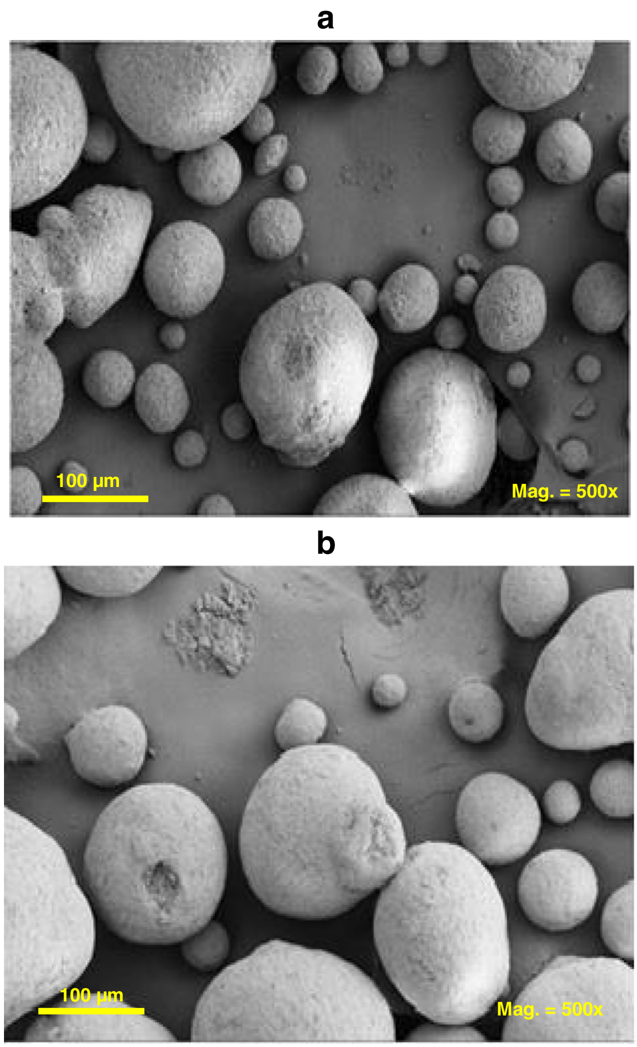

Fig. 2 Scanning electron microscope (SEM) pictures at magnification ×500 of **a** Pure NEU and **b** 9% APAP impregnated into NEU. The results indicated that there are no morphological changes after impregnation

good flow properties. SEM pictures of the impregnated product indicate that the morphological properties of the impregnated product are similar to pure NEU. The process of loading and drying of the drug particles within the carrier does not result in any discernable change in the external morphology of the carrier particles. There is no evidence of granulation, agglomeration, or coating of the carrier particles during the impregnation process.

The pure carrier is spherical in shape and the preservation of this sphericity is crucial for maintaining good flow properties of the carrier particles. The preservation of the particle size and morphology of the impregnated product by this method is a significant advantage over other impregnation processes such as co-grinding or milling of drugs with porous carriers [3, 6, 20], where strong attrition may lead to significant changes in surface morphology and particle-size distribution.

Shear Cell Tests

NEU US2 has good flow properties and compactibility, which are important in manufacturing of solid dosage forms, especially tablets. Flow properties of pharmaceutical solid powders are crucial requirements to successfully formulate them into final dosage forms. The flow properties of different impregnated products compared to pure NEU are shown in Fig. 3.

This figure is a plot of the measured shear stress vs. the applied normal stress. The resultant yield loci of the impregnated product are compared with pure NEU. The flow properties of the impregnated product are highly comparable to the flow properties of pure NEU. The data also suggests that the API has been successfully impregnated inside the NEU. If there is any APAP at the surface of NEU, this will result in a discernible change in the flow properties of the product mixture due to the largely poor flow properties of APAP as compared to NEU. However, our results showed a negligible effect of APAP impregnation on the flow properties of the final

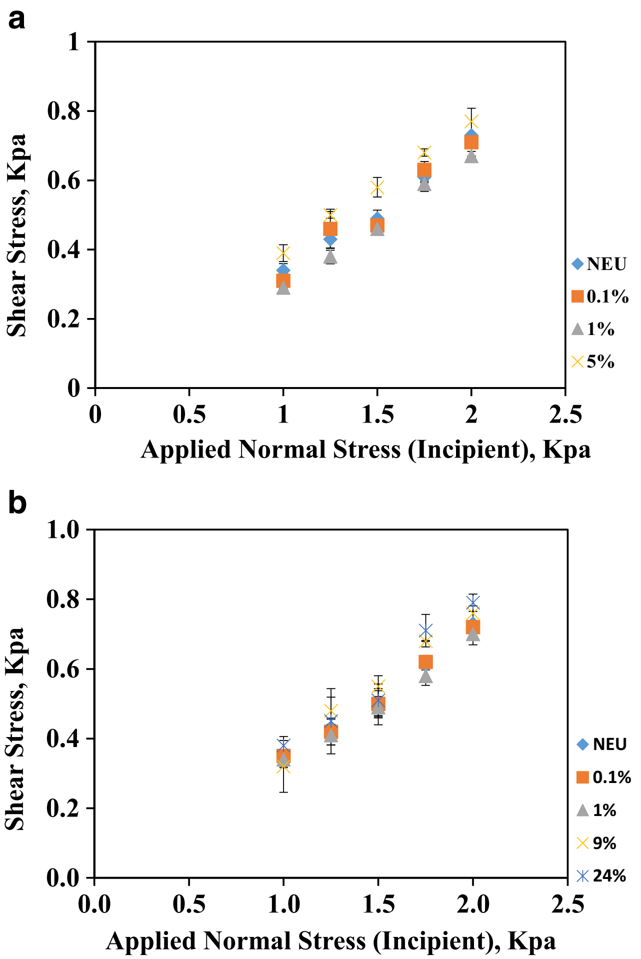

Fig. 3 FT4 Measurement of **a** pure Neusilin (NEU) and impregnated products using DI water as a solvent and **b** using methanol as a solvent. The good flow properties of the pure carrier are preserved even after impregnation

products. This suggests that there is no APAP at the surface of the impregnated products and the APAP has been placed inside the pores of the NEU. The result is in agreement with previous work on impregnation of API onto porous carriers [23]. The preservation of the flow properties of the pure NEU even after impregnation is an important advantage of this method, over other impregnation techniques.

Specific Surface Area and Pore Volume

The BET surface area and pore volume of pure and impregnated NEU are presented in Table 3 and Fig. 4. The surface area of NEU, which is determined using the BET method, was significantly reduced after being loaded with APAP. The free surface area of NEU before APAP loading was 390.4 m^2/g while it was 264.5 m^2/g and 226.8 m^2/g after loading with 5% and 24% APAP, respectively. This indicates that the surface area of 5% APAP loading represents about 67.8% of that of the pure NEU while the surface area of 24% APAP loading equals to 58.1% of the pure NEU. Results also revealed that the pore volume of pure NEU (1.742 cc/g) was higher before being loaded with 5% APAP (1.308 cc/g) and 24% APAP (1.091 cc/g), as expected.

These results indicate the impregnation of the drug particles within the carrier rather than external deposition. This study employs reduction in pore volume as an indicator of impregnation rather than reduction in pore size. This is because NEU has a very small pore size, around 5 nm, and these pores are irregular in shape. This makes it challenging to accurately quantify the reduction in pore size. Moreover, Gregg et al. [29] concluded that from the shape of BET curve, one can estimate the pore shape of porous carriers. This means that porous carriers with different pore shapes result in different BET behaviors. According to these findings, the pore shape of NEU is slit-type. Slit-type pores do not have regular dimensions. Therefore, it is better to depend on pore volume and not pore size in this study.

Loading and Blend Uniformity

Table 4 shows the results of loadings and blend uniformity for all impregnation experiments. The APAP loadings of all experiments are very close to their target loadings. This indicates that FB impregnation is successfully able to load APAP into NEU, with little APAP loss.

Table 3 BET studies for pure Neusilin and impregnated products. Pore volume and surface area were reduced after impregnation

Target loading	Surface area (m^2/g)	Total pore volume (cc/g)
Pure Neusilin	390.4	1.742
5%	264.5	1.308
24%	226.8	1.091

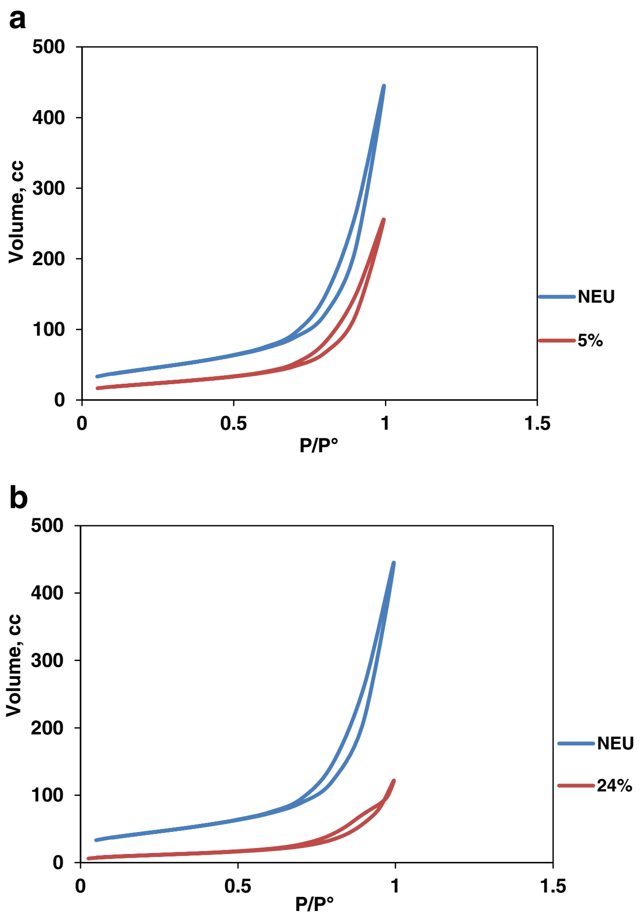

Fig. 4 BET curves for **a** pure Neusilin (NEU) and 5% APAP impregnated and **b** pure NEU and 24% IMP. There is a clear reduction in surface area after impregnation and it depends on APAP loading

FB impregnation produces a blend with high uniformity [23] and the results in this study confirmed that (see Table 4). The blend uniformity in this study was calculated as a relative standard deviation (%RSD). All impregnation experiments show a high blend uniformity with a RSD value of less than 5%. Achieving satisfactory blend uniformity can be challenging, especially for formulations with low API content. Using FB impregnation, satisfactory blend uniformity was achieved even for API loads as low as 0.1% and 1%. These results are in agreement with previous studies [23, 24].

Physical State of APAP Loaded into NEU

To study the state of APAP in the impregnated product, X-Ray diffraction of pure APAP, pure NEU, 5% APAP impregnated in NEU using DI water as a solvent, and 24% APAP impregnated in NEU using methanol as a solvent were conducted. The results are shown in Fig. 5.

Table 4 Blend uniformity of impregnated products. All impregnated products showed good blend uniformity

Target APAP (%)	Solvent	Average	RSD	C.I.
0.1	DI water	0.10	2.23	1.45–4.15
1		0.93	1.76	1.15–3.28
5		5.14	2.40	1.57–4.47
0.1	Methanol	0.11	4.27	2.76–7.94
1		1.05	3.02	1.97–5.62
9		8.21	4.43	2.88–8.24
24		24.28	2.68	1.74–4.98

The diffraction pattern of pure APAP presented a complete crystalline state while NEU US2 pattern showed a complete amorphous form. The crystalline form of APAP was confirmed by the appearance of several sharp peaks with high intensity: 11.97°, 13.64°, 15.37°, 16.54°, 18.03°, 18.78°, 20.25°, 23.32°, 24.20°, and 26.35° at 2 theta (θ) diffraction angle. Pure NEU showed a broad halo pattern, which confirms its amorphous structure. The diffraction pattern of 5% APAP in NEU resemble the pattern of pure NEU US2. These results thus indicate that APAP is converted into its amorphous state after being impregnated. The pattern of 24% APAP in NEU showed some small peaks with very low intensity: 26°, 24°, 23°, 18°, and 14° at 2 θ diffraction angle. Nevertheless, this pattern did not show any clear sign of APAP crystallinity. In general, the observed results of XRD study revealed that APAP exists mainly as an amorphous form in NEU.

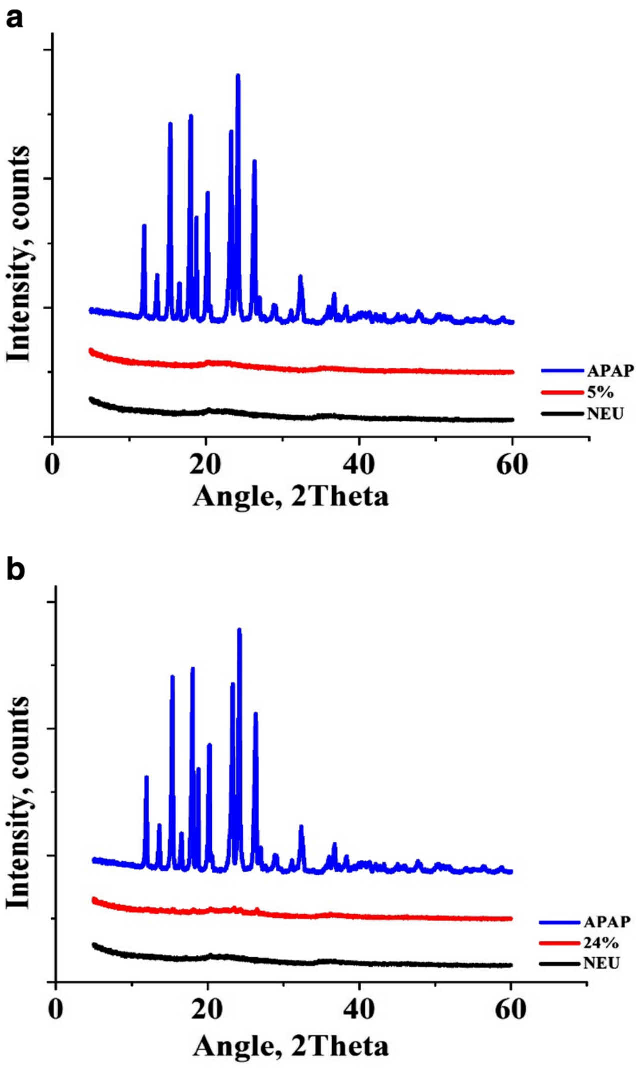

Fig. 5 PXRD of (a) pure APAP, pure Neusilin (NEU), and 5% APAP impregnated, and **b** pure APAP, pure NEU, and 24% APAP impregnated (IMP). The APAP in impregnated products presented an amorphous pattern

Similar findings were obtained from the Raman study which is presented in Fig. 6.

In Raman scattering study, we acquired the spectra from 200 to 1800 cm^{-1} for all samples. For APAP, many sharp peaks were observed in the regions of 790–900 cm^{-1} and 1200–1660 cm^{-1}. These regions were further elaborated into 797, 858, 1236, 1324, 1560, 1611, and 1649 cm^{-1}, which represent CNC ring stretching, ring breathing, C–C ring stretching, amide III, amide II, ring stretching, and amide I modes, respectively [30–32]. However, pure NEU showed no peaks. Five percent and 9% APAP in NEU have spectral pattern which resembles pure NEU (see Fig. 6a, b). On the other hand, the spectra of 24% APAP in NEU, as shown in Fig. 6 c revealed that there are very reduced peaks observed in the 790–900 cm^{-1} and 1200–1660 cm^{-1} regions. This difference in Raman spectra between 5%, 9%, and 24% APAP in NEU might indicate that there are a few crystals of APAP at the surface of NEU or within the NEU particles. In order to clarify these results, a physical mixture of 5%, 9%, and 24% APAP in NEU were prepared by using a Lab-ram mixer. Raman spectra of APAP and NEU physical blends were acquired because Raman data of 24% APAP in NEU showed some crystallinity while other characterization tests did not show such behavior. Figure 6 a, b showed that 5% and 9% physical mixtures of APAP in NEU have relatively sharp peaks in the 790–900 cm^{-1} and 1200–1660 cm^{-1} regions while impregnated products at the same concentrations do not show any significant peaks in these regions. On the other hand Fig. 6 c, demonstrated the differences in spectra of 24% impregnated NEU and the physical mixture. The physical mixture showed more intensified peaks at the same previously mentioned wave number regions. Also, peak intensities of the physical blends are dependent on the percentage of APAP while the impregnated products did not show such behavior. Although, the peak intensity of impregnated products was significantly lower than that the physical mixtures, the results indicate that for 24% APAP in NEU crystalline APAP could exist in the product. At the same time, the impregnation reduced the content of APAP in the crystalline form.

DSC is an efficient technique to study the state of solids. Appearance of phase transitions helps to recognize glassy

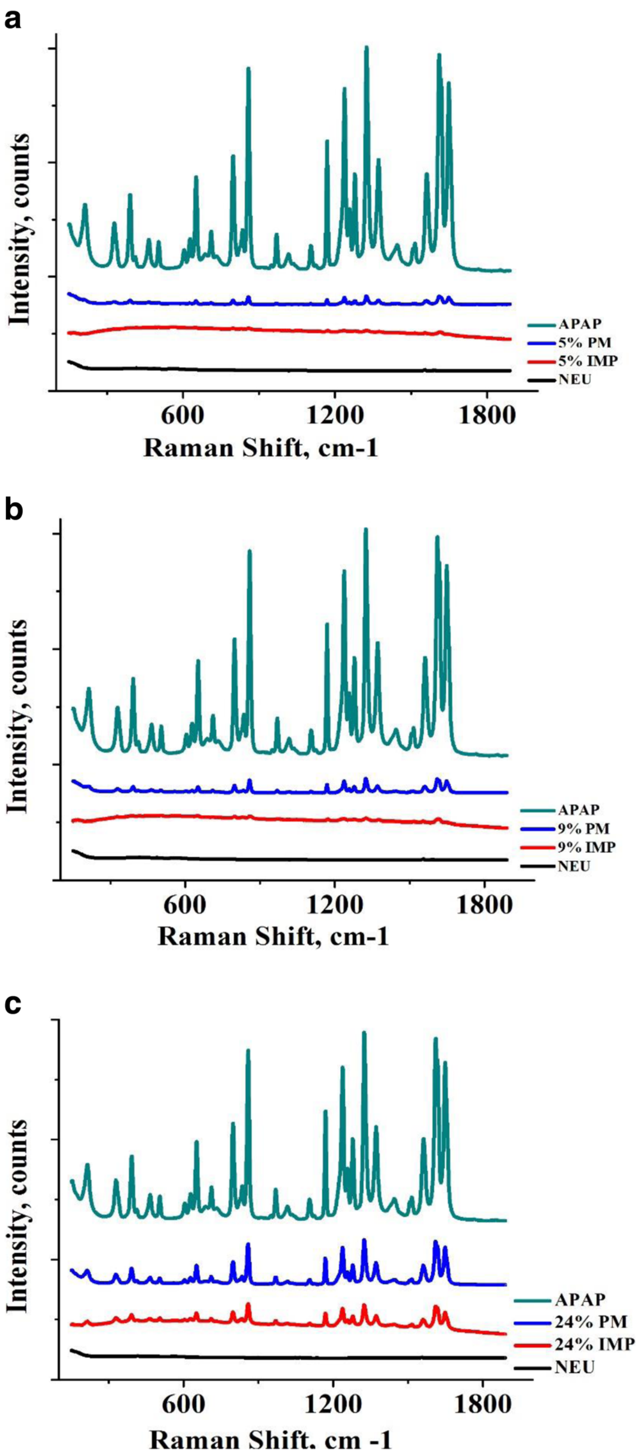

Fig. 6 Raman spectra of **a** pure APAP, pure Neusilin (NEU), 5% impregnated APAP (IMP), and 5% APAP physical mixture (PM). **b** Pure APAP, pure NEU, 9% impregnated APAP (IMP), and 9% APAP physical mixture (PM). **c** Pure APAP, pure NEU, 24% impregnated APAP (IMP), and 24% APAP physical mixture (PM). The results showed that APAP existed in amorphous form in impregnated products

from crystalline while disappearance of phase transitions means molecular dispersion (no peaks) of drugs within carriers. DSC curves are shown in Fig. 7 for pure and 5% and 24% of APAP impregnated in NEU. The DSC study of 1% APAP in NEU has not been conducted because we would not expect that the presence of tiny amounts of crystalline drugs in samples (10 mg) containing 1% APAP in NEU could be detected by DSC. From Fig. 7, it can be seen that pure APAP has a strong endothermic peak at 170 °C, which characterizes the melting point of crystalline APAP, while, pure NEU does not show any peak, which indicates its amorphous state. No peaks were also observed for 5% and 24% of APAP in NEU. The DSC curves resemble to a large extent that of pure NEU. The DSC results of impregnated products do not show any peaks (exothermic or/and endothermic) peaks in cooling (not shown) and heating data. The DSC results indicated that the drug is molecularly dispersed (no peaks in the DSC) in the NEU as has been explained by Mellaerts et al. [1]. For a molecular dispersion, the solid is in amorphous form, in which the intermolecular forces are broken down and the molecules are separately distributed within the carrier nano-pores. Thus, the formation of ordered structure and recrystallization are prevented by the confining effect of the pores. The results,

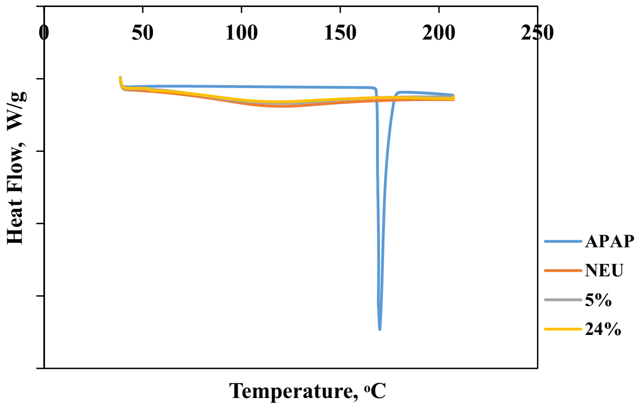

Fig. 7 Differential scanning calorimetry study of APAP, Neusilin (NEU), and 5% and 24% impregnated products. Pure APAP melted at 170 °C while NEU and impregnated products did not show any melting point

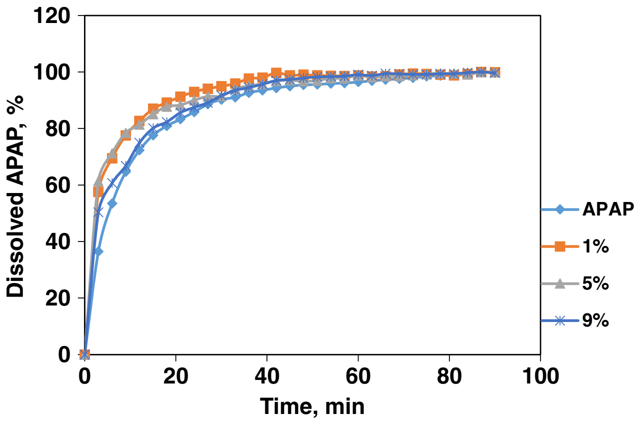

Fig. 8 Dissolution behavior of pure APAP and the impregnated product using DI water as a dissolution medium. One percent and 5% were prepared using DI water and 9% was prepared using methanol. No discernible differences are observed between the dissolution profiles

which are in agreement with XRD and Raman spectroscopy, further support the argument of amorphization of APAP during FB impregnation.

Drug Dissolution Behavior

The dissolution behavior of impregnated products was compared with the dissolution behavior of pure APAP using different dissolution media. Figure 8 shows the dissolution profiles of pure APAP and impregnated products in DI water.

The results indicate that there is no significant difference among the dissolution profiles of the samples in this dissolution medium. Impregnation of API onto a mesoporous carrier is expected to increase the dissolution rate of this API [8, 33] due to its amorphization during the process. However, in this study, the effect of impregnation on the dissolution behavior of the impregnated product is not discernible. APAP has a high solubility in the dissolution medium (DI water) making the profiles indistinguishable from pure APAP. However, the dissolution of impregnated APAP was enhanced in HCl, pH 1.2 media as shown in Fig. 9. Samples for Fig. 8 were tested over 100 min while samples for Fig. 9 were tested over 50 min because the dissolution rate of APAP using 0.1 N HCl as a dissolution medium was faster than the dissolution rates of APAP using DI water as a dissolution medium.

APAP does not show a pH-dependent solubility between a pH of 1.2 and 8.0 [34]. However, our results showed different dissolution behaviors of APAP in impregnated products using 0.1 N HCl and DI water as dissolution media. This is mainly due to that the improvement in the dissolution profiles of drug after loading it into silicate is not only due to amorphization. The release of silicic acid and ions (Mg^{2+} and Al^{3+}) from NEU into the dissolution medium significantly improves the dissolution rate of drugs. The release extent of these products is more in 0.1 N HCl than other dissolution medium [35]. In addition, the impregnated products in all dissolution media showed a constant rate in the late stage of dissolution, at which the change in the rate of dissolution tends to zero. This behavior might suggest that an interaction could exist between APAP molecules and the NEU (silanol group) in the impregnated products. A further study is needed to explore this interaction in more detail.

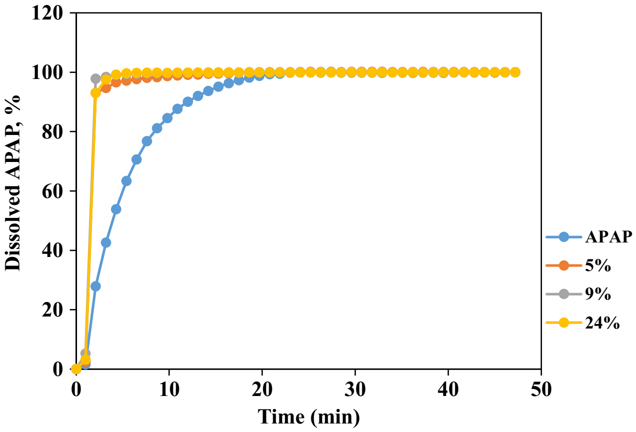

Fig. 9 Dissolution behavior of pure APAP and impregnated products using 0.1 N HCl as a dissolution medium. 5% product was prepared using DI water, and 9% and 24% were prepared using methanol. There is a clear difference between the dissolution profiles of pure APAP and impregnated products

Conclusions

In this study, a highly porous carrier (NEU) was successfully impregnated with acetaminophen in a fluidized bed. The resulting product was fully characterized, and the results demonstrated that these products have properties amenable for manufacturing as solid dosage forms. The impregnated product showed excellent blend uniformity, good flow properties, and a narrow particle-size distribution. In addition, the results indicated that the different evaporation profiles of the solvents do not affect the morphology or loading efficiency of APAP in NEU. Furthermore, the results showed that the blend uniformity did not depend on the drug loading or solvent type. The results also demonstrated that the APAP was present in the pores of the carrier mainly in its amorphous form. This was concluded from Raman spectroscopy, X-ray diffraction measurements, and DSC studies. Drug amorphization was observed because APAP is placed inside very fine pores (about 5 nm), which confined its dimensional growth, and prevented its recrystallization. This would be expected to improve APAP dissolution behavior in media where crystalline APAP shows poor solubility.

The use of a fluidized bed to impregnate APAP into porous carriers eliminates many unit operations in both drug and dosage form development. Application of fluidized bed impregnation in pharmaceutical manufacturing is a promising tool to decrease both downstream and upstream development efforts, which are necessary to adjust the properties of both drugs and dosage forms. However, additional work must be performed to study the effect of process parameters of the fluid bed operation on the properties of impregnated products. In addition, the conclusions of this work are based on one carrier and one drug substance and further work should be carried out to investigate the generality of our results. In particular, future work should investigate the feasibility of the method for other active ingredients and porous carriers. Moreover, we expect that co-impregnation of API and polymer would potentially alter the properties of the resulting materials and could control their release profiles. Future work should examine co-impregnation of API and polymer as a way to further control properties of the drug product.

Acknowledgements We like to thank Plamen Grigorov for assistance with some of the experiments. We would like to thank Pavithra Valliappan for the help with the writing of the manuscript.

Funding Information Some of the material in this paper is based upon the work supported by the National Science Foundation under Grant Number 1444903.

Compliance with ethical standards

Disclaimer Any opinions, findings, and conclusions or recommendations expressed in this material are those of the authors and do not necessarily reflect the views of the National Science Foundation.

References

1. Mellaerts R, Jammaer JAG, van Speybroeck M, Chen H, Humbeeck JV, Augustijns P, et al. Physical state of poorly water soluble therapeutic molecules loaded into SBA-15 ordered mesoporous silica carriers: a case study with itraconazole and ibuprofen. Langmuir. 2008;24(16):8651–9.
2. Song SW, Hidajat K, Kawi S. Functionalized SBA-15 materials as carriers for controlled drug delivery: influence of surface properties on matrix-drug interactions. Langmuir. 2005;21(21):9568–75.
3. Bouledjouidja A, Masmoudi Y, van Speybroeck M, Schueller L, Badens E. Impregnation of fenofibrate on mesoporous silica using supercritical carbon dioxide. Int J Pharm. 2016;499(1–2):1–9.
4. Kutza C, Metz H, Kutza J, Syrowatka F, Mäder K. Toward a detailed characterization of oil adsorbates as “solid liquids”. Eur J Pharm Biopharm. 2013;84(1):172–82.
5. Mura P, Valleri M, Cirri M, Mennini N. New solid self-microemulsifying systems to enhance dissolution rate of poorly water soluble drugs. Pharm Dev Technol. 2012;17(3):277–84.
6. Gupta MK, Vanwert A, Bogner RH. Formation of physically stable amorphous drugs by milling with Neusilin. J Pharm Sci. 2003;92(3):536–51.
7. Knapik J, Wojnarowska Z, Grzybowska K, Jurkiewicz K, Stankiewicz A, Paluch M. Stabilization of the amorphous ezetimibe drug by confining its dimension. Mol Pharm. 2016;13(4):1308–16.
8. Grigorov PI, Glasser BJ, Muzzio FJ. Improving dissolution kinetics of pharmaceuticals by fluidized bed impregnation of active pharmaceutical ingredients. AICHE J. 2016;62(12):4201–14.
9. Lemsi M, Galai H, Louhaichi MR, Fessi H, Kalfat R. Amorphization of atorvastatin calcium by mechanical process: characterization and stabilization within polymeric matrix. J Pharm Innov. 2017;12(3):216–25.
10. Wong WS, Lee CS, Er HM, Lim WH. Preparation and evaluation of palm oil-based polyesteramide solid dispersion for obtaining improved and targeted dissolution of mefenamic acid. J Pharm Innov. 2017;12(1):76–89.
11. Ambrogi V, Latterini L, Marmottini F, Tiralti MC, Ricci M. Oxybenzone entrapped in mesoporous silicate MCM-41. J Pharm Innov. 2013;8(4):212–7.
12. Qian KK, Bogner RH. Application of mesoporous silicon dioxide and silicate in oral amorphous drug delivery systems. J Pharm Sci. 2012;101(2):444–63.
13. Allgeier MC, Piper JL, Hinds J, Yates MH, Kolodsick KJ, Meury R, et al. Isolation and physical property optimization of an amorphous drug substance utilizing a high surface area magnesium aluminometasilicate (Neusilin((R)) US2). J Pharm Sci. 2016;105(10):3105–14.
14. Kinoshita M, Baba K, Nagayasu A, Yamabe K, Shimooka T, Takeichi Y’, et al. Improvement of solubility and oral bioavailability of a poorly water-soluble drug, TAS-301, by its melt-adsorption on a porous calcium silicate. J Pharm Sci. 2002;91(2):362–70.
15. Konno T, Kinuno K, Kataoka K. Physical and chemical changes of medicinals in mixtures with adsorbents in the solid state. I. Effect of vapor pressure of the medicinals on changes in crystalline properties. Chem Pharm Bull. 1986;34(1):301–7.
16. Qian KK, Suib SL, Bogner RH. Spontaneous crystalline-to-amorphous phase transformation of organic or medicinal compounds in the presence of porous media, part 2: Amorphization capacity and mechanisms of interaction. J Pharm Sci. 2011;100(11):4674–86.
17. Shen SC, Ng WK, Chia L, Dong YC, Tan RBH. Stabilized amorphous state of ibuprofen by co-spray drying with mesoporous SBA-15 to enhance dissolution properties. J Pharm Sci. 2010;99(4):1997–2007.
18. Mellaerts R, Mols R, Jammaer JAG, Aerts CA, Annaert P, van Humbeeck J, et al. Increasing the oral bioavailability of the poorly water soluble drug itraconazole with ordered mesoporous silica. Eur J Pharm Biopharm. 2008;69(1):223–30.
19. Van Speybroeck M, et al. Ordered mesoporous silica material SBA-15: a broad-spectrum formulation platform for poorly soluble drugs. J Pharm Sci. 2009;98(8):2648–58.
20. Mallick S, Pattnaik S, Swain K, de PK, Saha A, Ghoshal G, et al. Formation of physically stable amorphous phase of ibuprofen by solid state milling with kaolin. Eur J Pharm Biopharm. 2008;68(2):346–51.
21. Dhall M, Nanda S, Madan AK. Studies on flash evaporation for preparation of porous solid dispersions using piroxicam as a model drug. J Pharm Innov. 2011;6(4):232–40.
22. Charnay C, Bégu S, Tourné-Péteilh C, Nicole L, Lerner DA, Devoisselle JM. Inclusion of ibuprofen in mesoporous templated silica: drug loading and release property. Eur J Pharm Biopharm. 2004;57(3):533–40.
23. Grigorov PI, Glasser BJ, Muzzio FJ. Formulation and manufacture of pharmaceuticals by fluidized-bed impregnation of active pharmaceutical ingredients onto porous carriers. AICHE J. 2013;59(12):4538–52.
24. Carson JW, Wilms H. Development of an international standard for shear testing. Powder Technol. 2006;167:1–9.
25. Freeman R. Measuring the flow properties of consolidated, conditioned and aerated powders - a comparative study using a powder rheometer and a rotational shear cell. Powder Technol. 2007;174(1–2):25–33.
26. Brunauer S, Emmett PH, Teller E. Adsorption of gases in multimolecular layers. J Am Chem Soc. 1938;60(2):309–19.
27. Gao Y, Ierapetritou MG, Muzzio FJ. Determination of the confidence interval of the relative standard deviation using convolution. J Pharm Innov. 2013;8(2):72–82.
28. Oka S, Sahay A, Meng W, Muzzio F. Diminished segregation in continuous powder mixing. Powder Technol. 2017;309:79–88.
29. Greggy SJ, Sing KSW. Adsorption, Surface Area, and Porosity: Academic Press Inc (London) Ltd; 1982. Appendix.
30. Dollish FR, Fateley WG, Bentley FF. Characteristic Raman frequencies of organic compounds. New YorkUSA: Wiley; 1974. Appendix One
31. Diniz JEM, Borges RS, Alves CNA. DFT study for paracetamol and 3, 5-disubstituted analogues. J Mol Struct Theochem. 2004;673:93–7.
32. Hernández B, Pflüger F, Kruglik SG, Ghomi M. Characteristic Raman lines of phenylalanine analyzed by a multiconformational approach. J Raman Spectrosc. 2013;44(6):827–33.
33. Mellaerts R, Aerts CA, Humbeeck JV, Augustijns P, den Mooter GV, Martens JA. Enhanced release of itraconazole from ordered mesoporous SBA-15 silica materials. Chem Commun (Camb). 2007;(13):1375–7.

34. Shaw LR, Irwin WJ, Grattan TJ, Conway BR. The effect of selected water-soluble excipients on the dissolution of paracetamol and ibuprofen. Drug Dev Ind Pharm. 2005;31(6):515–25.
35. Bahl D, Bogner RH. Amorphization alone does not account for the enhancement of solubility of drug co-ground with silicate: the case of indomethacin. AAPS PharmSciTech. 2008;9(1):146–53.